

CHALLENGES IN GEOMETRY DEVELOPMENT FOR THE CRM-HL ECOSYSTEM

Adam M. Clark¹ & Doug S. Lacy¹

¹Boeing Commercial Airplanes

Abstract

In 2014, the High-Lift Common Research model (CRM-HL) geometry was developed by Boeing and made publicly available to initially support efforts at NASA to develop advanced aerodynamic technologies. Since then, further development has occurred to define a reference set of geometry CAD files and configurations of interest, including cruise, takeoff, landing, and associated small perturbations to challenge CFD validation exercises. These development efforts have enabled the formation a robust international "ecosystem", with its foundation centered around the building, experimental testing, and computational simulations of several CRM-HL models of different scales by various partners around the world. Ensuring that the physical models developed are a faithful representative of the reference CRM-HL configurations presents unique challenges. Additionally, accurate and robust CFD simulation that match the physical experiments requires specific focus and attention to geometric detail. This paper will discuss the geometric considerations for consistent development and experimental testing of the CRM-HL configurations, as well as highlight requirements for CFD modeling across the CRM-HL ecosystem.

Keywords: CRM-HL, Aerodynamics, Validation, Experimental Testing, CFD

Nomenclature

λ	Wing Taper Ratio	S_{ref}	Wing Reference Area
$\Lambda_{\text{C/4}}$	Sweep at 1/4 Chord	WRP	Wing Reference Plane
AR	Wing Aspect Ratio	X_{ref}	Moment Reference Center (X)
C_{ref}	Wing Reference Chord	\mathbf{Y}_{ref}	Moment Reference Center (Y)
LES	Leading Edge Coordinate System	Z_{ref}	Moment Reference Center (Z)

1. Introduction

The High Lift Common Research Model (CRM-HL) was initially designed in 2016 to provide a modern, industrially-relevant platform that could be used for aerodynamic technology development and computational fluid dynamics (CFD) validation [1] without restrictions on distribution due to intellectual property concerns. Since its inception, the CRM-HL Ecosystem has flourished with participation

from NASA, Boeing, ONERA, Kawasaki Heavy Industries, JAXA, and several other partners, resulting in at least four wind-tunnel models and a dozen test campaigns, with several additional models and many more tests planned in the near future. In addition to being used as facility check and/or standard models in many cases, ecosystem testing of the CRM-HL models will specifically explore high-lift flow physics up to flight Reynolds numbers and advance wind tunnel testing techniques, while contributing to a global body of data that can be synthesized and cross-plotted to gain insights into facility to facility and model to model differences. In this regard, it is paramount to ensure that all models are designed and built to the same geometric specifications to ensure the highest degree of aerodynamic similarity possible.

The geometry specifications for the CRM-HL are defined such that representative and relevant flow features of interest that can be consistently studied both in a wind tunnel and computationally. Configuration variations enable the capability to isolate key features or combine them as makes sense to enhance study efficiency and effectiveness. In addition to configuration variations, the geometry is designed such that variations in shape and positioning of the high-lift elements are feasible, such that trends can be evaluated systematically, which if validated in CFD, is a critical step towards optimization.

The CRM-HL model is specified as a set of geometric surface lofts that fully define each unique external surface, and positioning information, which allows surfaces to be provided in the coordinate system most appropriate to manufacture or setup, then positioned into the global airplane coordinate system. The geometry computer aided design (CAD) files are hosted by NASA [2] and openly available. A specific collection of the surface lofts, along with definitions of end planes, trim surfaces, and positioning information fully define a specific reference configuration. Beyond the reference configuration definition, a number of aerodynamically important details remain incompletely defined, including specific surface component sealing considerations, slat bracket locations and size (which are function of model loads and therefore differ from model to model), and pressure port definitions. Many of these details have been informally communicated to ecosystem partners as models were designed, and are documented in Section 2.

High lift geometry is inherently very complex, which increases the risk of unintentional differences between different representations of the same configuration. Once a model is designed but prior to fabrication, it is critical to compare the as-designed CAD to the reference geometry. Over the course of several ecosystem model designs, several discrepancies have been detected this way either due to lack of definition in the reference configurations or geometry that had been revised after designs are complete. In doing so, designs can either be revised before manufacture, or known geometric discrepancies can be documented for future uses, particularly if the CAD or physical model are used in comparison with other models within the ecosystem. After fabrication, verification that the asbuilt geometry matches the intent is also required. Verification can be performed through a formal inspection process, which typically results in a comprehensive inspection report. Verification can be performed on an individual part, or on assemblies, or both. It is further recommended that key specifications that drive aerodynamic performance are verified independently. Predominantly, this involves measuring the physical gaps between the main wing element and flaps and slats. Details on these requirements are provided in Section 3.

Finally, given that one of the primary purposes of the CRM-HL ecosystem is CFD validation, there are several considerations necessary when generating geometry specific to CFD. Often, CFD geometry is built from the as-designed parts which requires significant effort to combine and simplify CAD pieces such that extraneous geometric details such as fastener holes and part breaks are removed. Section 4describes an approach where consistent CFD models are built from the reference geometry with model specific details added, such as slat brackets. This results in a set of comparable high-quality geometric models across the ecosystem that can easily be consistently utilized for a variety of purposes.

2. Further Reference Configuration Details

2.1 Reference Configurations

Following the original development of the CRM-HL geometry [1], NASA fabricated a 10% scale model which was initially tested at the 14x22 Foot [3] wind tunnel at NASA Langley Research Center, but then was subsequently tested at the QinetiQ 5-meter (Q5m) Wind Tunnel in Farnborough, UK [4] to specifically develop the reference landing and takeoff configurations. These configurations are thoroughly documented by Lacy [5] and represent the full geometric complexity available in the reference geometry, including leading edge slats, trailing edge flaps, a nacelle, and a pylon. The wing in the reference landing configuration is shown in Figure 1.

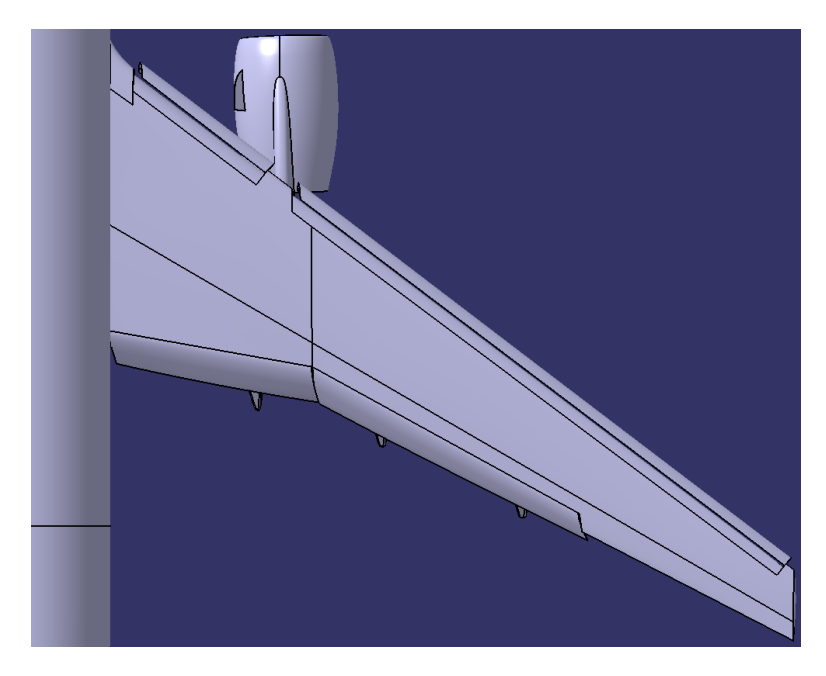


Figure 1 – CRM-HL Reference Landing Configuration

Beyond the full reference landing and takeoff configurations, the CRM-HL geometry is extremely modular, and is deliberately provisioned to systematically explore simplified configuration flow physics. Simplifications include testing the model with and without the empennage, nacelle/pylon, and landing gear, for instance. Simplified configurations like these have been extensively tested in a number of wind tunnel tests including at the Q5m with the NASA 10% semi-span model [4], at the ONERA F1 with a 5.1% full-span model [6], and most recently at the NASA National Transonic Facility (NTF) with a 5.2% semi-span model. Additionally, testing of these modular build-up configurations enable systematic CFD validation by gradually exposing separate elements of high-lift flow physics, as opposed to trying to uncouple the complex flow physics interactions present on the full landing configuration. The focus on CFD validation of the CRM-HL configuration buildup is one of the test cases posed for the 2024 American Institute of Aeronautics and Astronautics 5th High Lift Prediction Workshop (AIAA HLPW5).

The most basic configuration with the CRM-HL geometry mimics the original transonic Common Research Model [7], and consists of the fuselage, CRM-HL wing and flap support fairings (FSFs). It should be noted that the CRM-HL wing loft differs from the transonic CRM loft as described by Lacy [1], although it retains the same overall planform. This most basic configuration is referred to as the CRM-HL wing-body configuration (CRM-HL-WB) and is depicted in Figure 2.

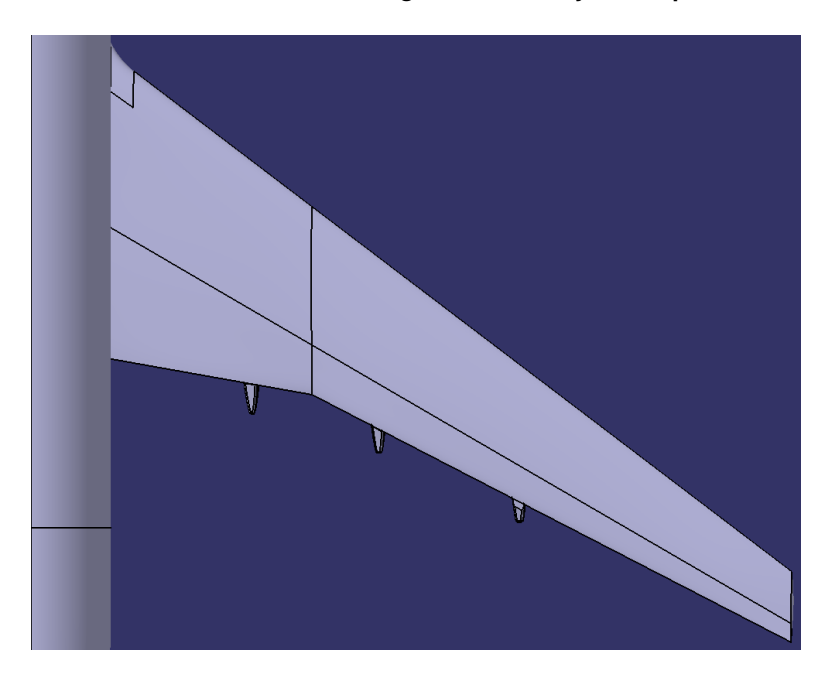


Figure 2 – CRM-HL-WB Configuration

Building on the CRM-HL-WB configuration, complexity is added to bring the configuration closer to a full high lift configuration. The Wing-Body-Slat configuration (CRM-HL-WBS) takes a first step in adding a continuous leading edge slat, spanning the location where the nacelle will eventually sit. It is important to note that although this configuration feature leading edge slats, it does not include slat brackets in the reference definition. Bracket definitions are unique to particular models, and can be added to make model specific CRM-HL-WBS configurations. The reference CRM-HL-WBS configuration is shown in Figure 3.

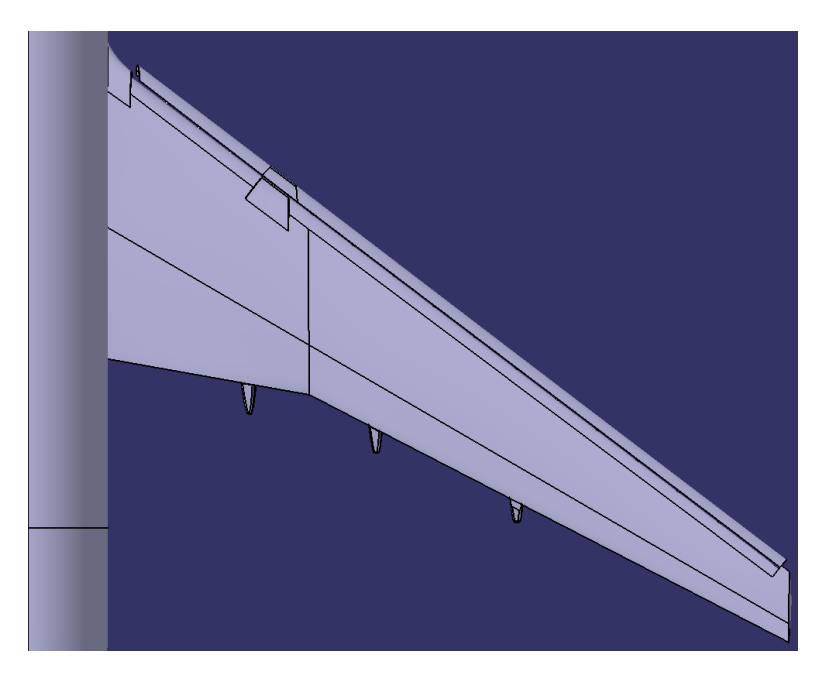


Figure 3 – CRM-HL-WBS Configuration

Next, the full trailing edge flap system is added to increase lift in the linear region, and bring the configuration closer to the reference landing configuration. This is known as the wing-body-slat-flap configuration (CRM-HL-WBSF) and is shown in figure 4. Finally, the continuous slat can be split, and the nacelle added to bring the model up to the reference landing configuration.

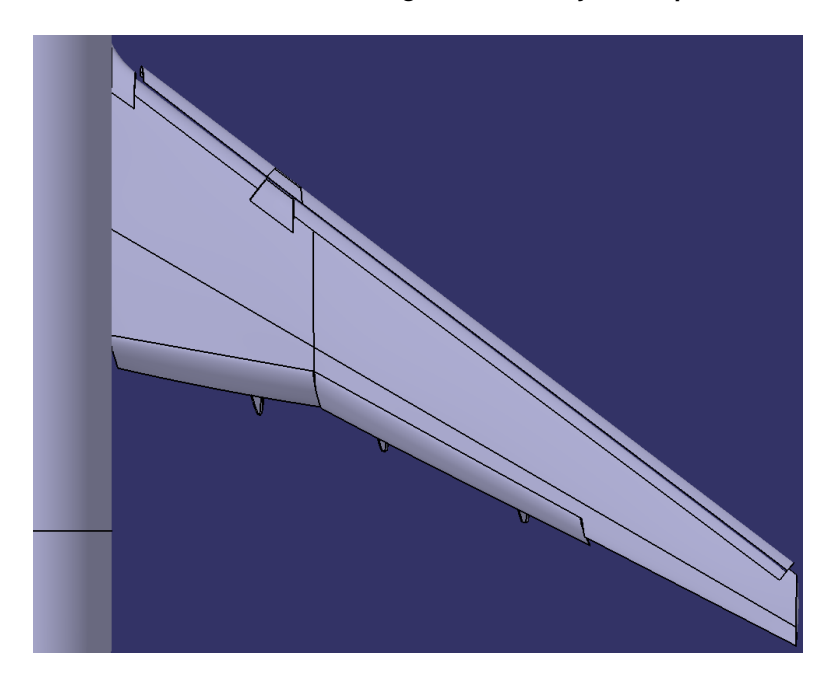


Figure 4 – CRM-HL-WBSF Configuration

Beyond the build-up configurations a few other noteworthy configurations have been studied. As part of the Q5m test campaign [4], a series of alternate flap deflections were studied and subsequently utilized as a test case for AIAA HLPW4 [8]. These configurations perturb the inboard and outboard flaps by 3° in both directions. While the reference landing configuration features a 40° deflected inboard flap and a 37° deflected outboard flap, the increased deflection variant features inboard and outboard flaps at 43° and 40° respectively, and the decreased deflection variant sets them to 37° and 34° respectively. These configurations are particularly valuable in assessing CFD capabilities with respect to flap performance, as well as providing a lower flap deflection that is more meaningfully attached at lower Reynolds numbers. It is expected that the decreased deflection configuration will be widely used with smaller, lower Reynolds number models. Lastly, the reference landing configuration without a Nacelle chine is of interest to isolate the impacts of the chine vortex in the same manner as the reference build up configurations. This configuration has been tested across several facilities to date. These configurations are highlighted as they represent some of the interesting variations that can be explored with the CRM-HL geometry, though there are many more.

2.2 Slat Bracket Definitions

The description and rationale of slat bracket size and shape are discussed extensively by Lacy in the original reference configuration definition paper [5]. A typical interpretation of those requirements is shown in the CAD geometry of the ONERA F1 model in Figure 5. It is worth stressing that the high energy flow that passes through the gap between the slat and the main element must flow around the slat brackets, and thus they can have an outsized impact on the aerodynamic characteristics of the wing. A typical wake behind slat brackets on the outboard wing is shown in Figure 6. Because the slat brackets have the potential to affect airplane level aerodynamics, it is critical to define them as consistently as possible between ecosystem models. In designing a new model, comparisons should be made to other ecosystem models using the configuration specific geometry found on the NASA Common Research Model webpage [2].

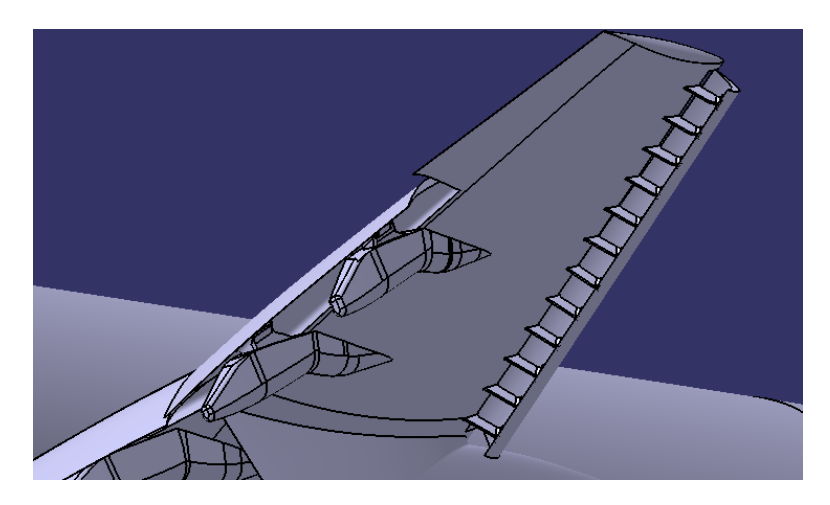


Figure 5 – ONERA Designed Slat Brackets on CRM-HL

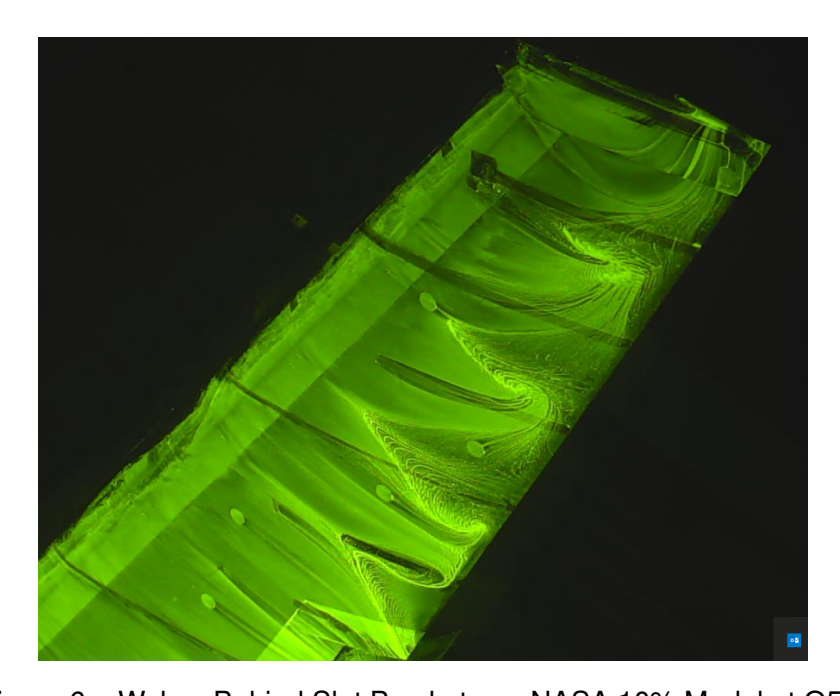


Figure 6 – Wakes Behind Slat Brackets on NASA 10% Model at Q5m

Further guidance is provided by Lacy [5] as to the locations and shape of the slat brackets, however reference locations of exact bracket centerlines were passed to model designers informally. Reference locations for the slat brackets in Leading Edge Coordinates are provided in Tables 1 and 2, which are further described by Lacy and provided consistent with the reference geometry dataset.

Table 1 – Inboard Slat Bracket Locations in LES

IB	Mid	ОВ
269.63	331.09	392.54

Even with leading edge bracket centerline locations, desired bracket width, and positioning requirements provided, small geometric variations are still expected around leading edge attachment hardware. Some variation may exist around where the leading edge brackets intersect the wing lower surface for example, due to differences in bracket cross-section, perhaps to provision for slat positioning adjustability. To account for some of this, leading edge brackets attach to the wing in pockets that are typically covered with plates. Any remaining gaps can lead to contour or sealing imperfections, and should be taped over and sealed.

Table 2 – Outboard Slat Bracket Locations in LES

Slat 6 IB 549.39	Slat 6 OB 627.01	 Slat 5 OB 782.25	 Slat 4 OB 937.48
	Slat 3 OB 1092.72	 	

On the trailing edge, flap support fairing geometry is provided to aerodynamically reduce the impact of flap support hardware. This fairing features a forward portion that is fixed to the wing, an aft portion that deflects downward about a hinge line, and a surface that blends the two together. The downward deflection of the aft portion of the flap support fairing is different from the actual flap deflection, and captured in Table 3. Aside from the fairing loft, minimal guidance is provided beyond requiring brackets to fit within the aerodynamic fairings, and keeping the bracket mounting pad on the flap aft of the expected attachment line. This guidance is enough to provide required flexibility in model architecture, and limit differences to areas that aren't aerodynamically significant.

Table 3 – Flap Support Fairing Deflections

Flap Deflection	IB Fairing Deflection	OB Fairing Deflection
10°	9.0°	8.0°
25°	19.0°	17.0°
34°	N/A	21.5°
37°	26.0°	24.0°
40°	29.0°	26.5°
43°	32.0°	N/A

2.3 Sealing Guidance

The spanwise edges between the inboard and outboard flaps are defined in the reference CAD and are trimmed to provide sufficient clearance through all detents, as can be seen in Figure 7. On a typical flight configuration, these surfaces would be sealed together using flexible seals to maximize performance. However, due to the range of different inboard and outboard deflections defined for the CRM-HL, sealing the full chord is impossible. Models designed and tested to date have provided various methods to seal this junction, typically using tape and a moldable filler. In order to maintain consistency across models and tests, a common size specification is necessary. Here, the distance is measured on the lower side along the surface of the flap, and is specified as 42" full-scale from the trailing-edge of the inboard flap forward to the leading edge for landing flap detents, and 24" full-scale for takeoff detents (F10, F25). The top surface should be filled and faired to minimize the leading-edge spanwise discontinuity. One example of this is shown in Figure 8. The inboard flap to fuselage sealing is defined by the piece of flap that extends into the body for structural support. This extent is specified by the trim planes associated with the inboard flap loft.

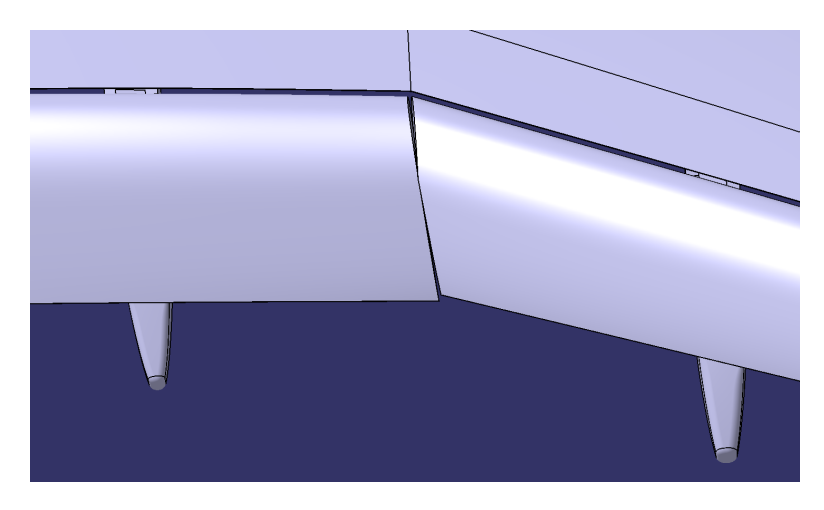


Figure 7 – Inboard to Outboard Flap Junction in Reference CAD



Figure 8 - Inboard to Outboard Flap Junction as tested in QinteiQ on the NASA 10% model

2.4 Pressure Port Definitions

As described by Lacy [5], reference pressure belt locations are defined across the wing as shown in Figure 9. A single pressure belt features a forward portion that is normal to the wing leading edge until it transitions to constant Y locations at the wing quarter-chord. Belts are further defined to be normal to the wing reference plane (WRP). These pressure belts have been adopted by ecosystem partners with minimal adjustments to spanwise location and chordwise distributions on all models built to date, and have been used extensively for comparison within the context of AIAA HLPW 4 and 5. Slat and flap pressure belts are additionally specified to match the wing belts in the stowed configuration, but move out of plane as the surfaces are deployed. Reference pressure belt locations are specified in Appendix A. It is noted that some deviations naturally arise from the reference locations in most all models due to considerations for specific test requirements, or in the quantity of belts available due to structural considerations, however it is the intent to have as much commonality in tap locations across models. Exact pressure tap layouts for each of the models in the ecosystem are not captured here, though they can be found in documentation associated with each specific model.

In addition to static pressure ports, a series of reference dynamic pressure port locations are specified, again shown in Appendix A. Locations for these ports were chosen to collect data at features

of interest, such as flow unsteadiness behind a slat bracket or on the wing tip. Several models were built with dynamic pressure transducers at most, if not all, of these locations, including the NASA 5.2%, NASA 2.7%, and Boeing 6%. Beyond the reference dynamic pressure ports, it is expected that individual models will adopt unique measurement locations specific to their requirements.

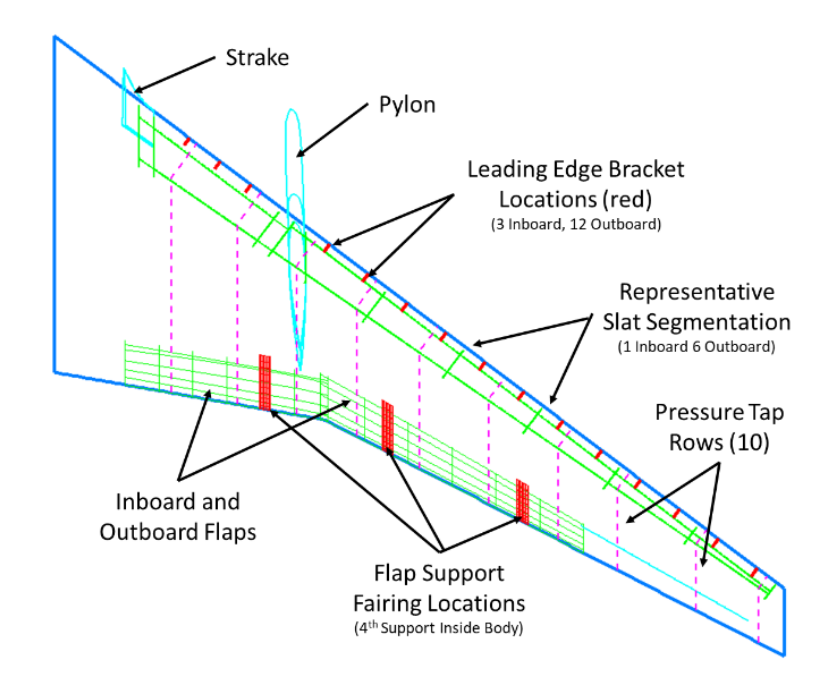


Figure 9 – Pressure Rows Defined on Wing

2.5 Model Tripping

Given the wide range of Reynolds number expected to be tested across the CRM-HL ecosystem, a consistent laminar to turbulent tripping strategy is necessary to produce comparable results across facilities. Tripping devices are generally used to fix the boundary-layer transition from laminar to turbulent flow in wind tunnel experiments. This generally involves applying physical trip strips (often referred to as trip dots or Cadcut strips) to key regions. For the full CRM-HL region, these regions include the fuselage nose, the nacelle inside and outside, the very limited region of the wing that is unprotected by leading edge devices, and the full empennage. High lift devices including slats and flaps are left to transition naturally because their strong pressure gradients provide quantifiable and consistent natural transition locations, and physical tripping if done incorrectly can be detrimental to performance. In the intermediate build-up configurations described in Section 2.1, tripping extent is adjusted to match the unprotected wing area, meaning that the trips on the wing over the nacelle are removed in the CRM-HL-WBSF configuration, but the full wing is tripped for the CRM-HL-WB configuration. Curves aligned with the trip locations are provided alongside the reference geometry [2], and are shown in Figure 10 on the full landing configuration.

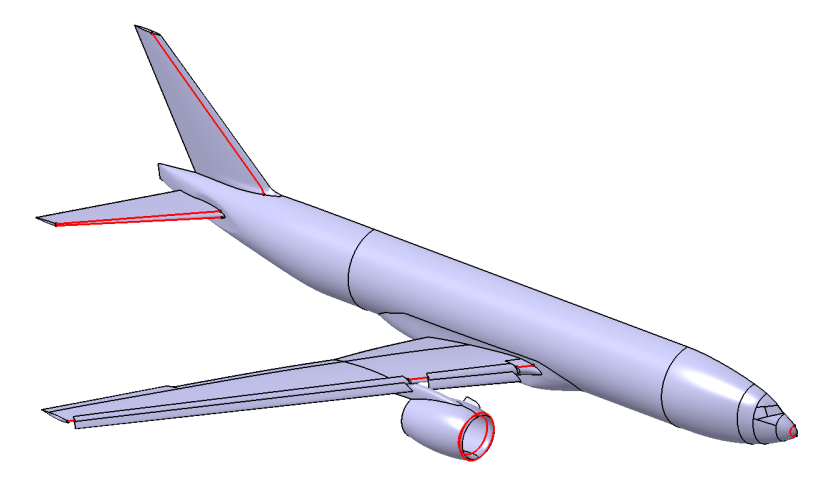


Figure 10 – Trip Locations Highlighted in Red on the CRM-HL-LDG configuration

Although tripping locations are explicitly specified and expected to remain constant across models, tripping device sizing is left to be defined by each test facility, as they are typically adjusted to match the facility best practices and Reynolds numbers achievable on test. For example, the trip dots used on the NASA 10% scale model tested at QinetiQ consisted of circular dots with a height of 0.01 inches, a diameter of 0.05 inches, and spaced at 0.10 inches, while trips used at the ONERA F1 on a smaller model were 0.005 inches in height to better match the model size and facility. At the National Transonic Facility, the model was left untripped at the highest Reynolds numbers.

2.6 Reference Values

Given that the CRM-HL was defined based on a small modification of the original transonic CRM [7], reference quantities are chosen to be consistent between the high-lift and transonic configurations. They are repeated in Table 4 below in for the full-scale, full-span airplane.

Table 4 – CRM-HL Reference Values, in body coordinates

S _{ref}	594,720.0 in ²
C_{ref}	275.80.0 in
Span	2,313.50 in
X_{ref}	1,325.90 in
Y_{ref}	468.75 in
Z_{ref}	177.95 in
λ	0.275
$\Lambda_{C/4}$	35°
AR	9.0

2.7 Alternate Trailing Edge Thickness

The baseline set of CRM-HL reference geometry includes surfaces with trailing edge thickness values of 0.20" full-scale, which yields a 0.01" trailing edge thickness on a 5% scale model. While this is adequate for many of the larger models within the CRM-HL ecosystem, a number of smaller scale models are planned for use in smaller wind-tunnels. As the model scale drops below 5%, the trailing edge thickness can become too thin to reasonably manufacture. In order to maintain consistency across the ecosystem, a family of reference geometry is defined that includes trailing edge thicknesses of 0.40", which is valid for models down to approximately 2% scale. Beyond the trailing edge thickness changes, flap and slat positions are also slightly modified to maintain the same

gap as set on the thin trailing edge family. Leading edge contours, including that of the wing under slat surface are left unchanged for this family of geometry.

2.8 Reference Configuration Deviations

It is worth highlighting that a full definition of the CRM-HL reference configuration was not available from the outset. Rather, an initial geometry was defined, and then refined over a series of wind-tunnel tests spanning years. As a result, there are some noteworthy geometry differences from test to test and model to model, particularly in the earlier models and tests. Additionally, some computational studies were launched in the interim, and have continued to rely on testing using the preliminary reference configuration in order to be consistent with the early data collected. When comparing data from test to test, it is important to understand all of the geometric differences that could have aerodynamic impacts. First, we note the following differences between the preliminary reference configuration and final reference configurations:

- Original transonic CRM nacelle lip shape changed (reshaped to reduce flow separate at high angles of attack)
- · Trailing edge flap positioning optimized
- · Leading edge slat positioning optimized
- Wing under-slat surface loft changed (reshaped to allow slat in final reference configuration take-off position to physically seal across the span)
- · Chine position optimized

Since the changes between the preliminary reference configuration and the final reference configuration include surfaces that are reshaped, it is worth highlighting some of the model differences relative to the final configuration. Notable differences between models and the final configuration are listed in Table 5

To fully capture the geometrical variations in circulation, we also need to document which models and configurations are used for the major workshops supported by the CRM-HL to-date. These configurations represent widely circulated CFD geometry. These are shown in 6

Table 5 – CRM-HL Geometry Variations in Models

Wind-Tunnel Model	Differences from Final Reference
NASA 10% Model	Preliminary nacelle contour
	Preliminary WUSS contours (IB and OB)
	Both preliminary and representative final reference positioning are tested
	 Spoiler trailing edge trim mismatch due to error, flaps properly positioned relative to as-built spoiler trailing edges
	Adjustable chine position. Both Final and Preliminary positions tested
	Flap track fairings are a different loft than final reference
ONERA LRM-HL	 Legacy fuselage with some smoothing around windshield and wing-body- fairing
	Very minor nacelle chine position difference
	Minor pylon lower surface trim change
	 WUSS uses preliminary geometry, but slat maintains proper reference takeoff positioning
	Minor flap to flap and flap to fuselage sealing differences
	 Flap track fairings are based off of 10% design, not reference design
KHI 3.23%	Flap track fairings are based off of 10% design, not reference design
	Uses 0.40" TE thickness geometry
NASA 5.2%	Very minor nacelle chine position difference
	 Flap track fairings are based off of 10% design, not reference design
Boeing 6.0%	No known discrepancies

Table 6 - CRM-HL Geometry as used in Workshops

Workshop	Model and Configuration
AIAA HLPW-3	CRM-HL-WBSF Preliminary Reference Configuration
AIAA HLPW-4	NASA 10% Model, Final Reference Configuration
AIAA HLPW-5	Test Case 1: CRM-HL Wing Body (Reference Geometry)
	• Test Case 2: ONERA LRM-HL, WB, WBS, WBSF, LDG Final Reference Config.
	Test Case 3: NASA 5.2%, Final Reference Configuration

3. Model and Design Verification

As discussed in Section 2, in order to successfully compare results from multiple wind-tunnel models across the CRM-HL ecosystem, a consistent and documented definition of all aspects of the model design and fabrication is paramount. Beyond providing a comprehensive definition of the external shape of the vehicle, detailed geometric verification of the design is necessary in order to minimize uncertainty in model build. Only in doing so is one able to draw technical conclusions about parameters of interest, such as Reynolds number sensitivities across a wide range models and test facilities, or sensitivities due to the particulars of tunnel interference. This verification should happen both before the model is fabricated by ensuring the as-designed assemblies closely match the reference geometry, and after fabrication by comparing the as-built article to the as-designed assembly. Both aspects of verification should be documented, understood, and generally made available to those using the experimental data collected using a specific test article.

3.1 Design Verification

While every effort is made to provide as consistent of a geometric definition as possible across models, specific facility or model design requirements, which may lie outside of the scope of the Ecosystem, can drive differences. For example, a requirement to test leading edge slat or trailing edge flap positions beyond the range designed within the ecosystem could drive differences in trim plane locations in order to avoid part to part interference. In addition to requirement-driven design deviations, a few models were designed prior to the final geometry definition. Notably, this includes the NASA 10% model and the ONERA 1/19.5 Large Reference Model (LRM). The NASA model was used to define the final reference configuration [4] [5], and as such, updates to the outboard wing under-slat-surface, and to the nacelle lip contour were made as a result of the preliminary testing. On the ONERA LRM, schedule issues prevented incorporation of the final configurations of the final wing under-slat-surface and flap track fairings [6]. With both models, the deviations are understood to be aerodynamically minor, and documented.

In order to properly compare a particular model design to the reference configuration, it is recommended to use the published reference CAD definitions provided within the CRM-HL ecosystem [2], and overlay the appropriately scaled wind-tunnel model assembly. In doing so, edges of parts can be inspected to identify any trim plane differences and/or contour differences from incorrectly translated surfaces. Any noted discrepancies should then be communicated and documented. An example of these comparisons is depicted in Figures 11 and 12 where cross-hatched colors show multiple surfaces that adhere to the same underlying geometry, and solid color contours indicate surface geometry differences.

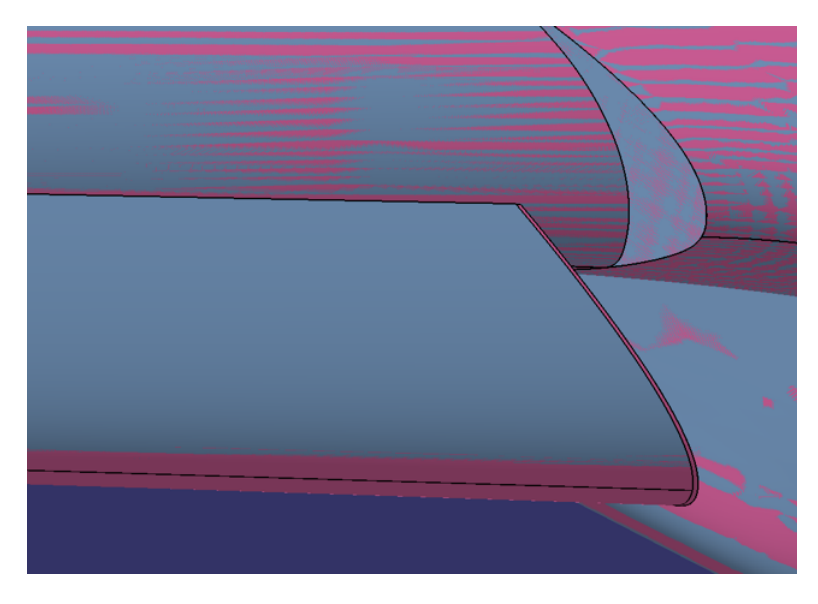


Figure 11 – Reference Configuration (Grey) Compared to ONERA LRM (Pink) Highlighting Minor Inboard Slat Trim Plane Difference, Due to Late Reference Configuration Update

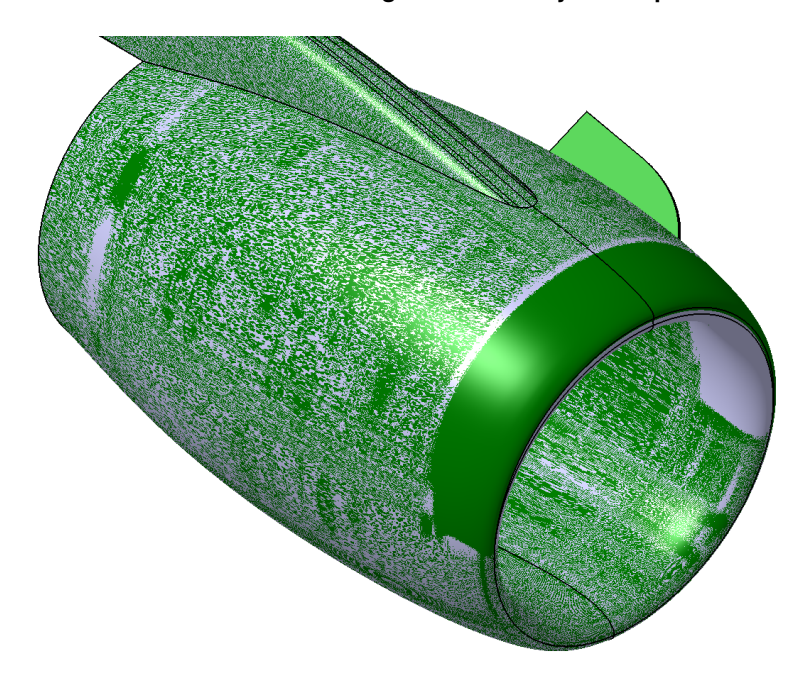


Figure 12 – Reference Configuration (Grey) compared to NASA 10% Model (Green) Highlighting Nacelle Re-contouring

An alternative and more quantitative approach may involve discretizing the external surface of the reference geometry into points, then comparing the distance of the points to the as-designed model CAD. Additional tools may be available to automate this approach within particular CAD tools. These approaches would equivalently highlight differences between the two models, but also provide a set of discrete distances from which statistics for the model could be calculated. While often a rigorous quantitative approach can be desired, using an overlay approach then spot-checking deviations found to quantify them is sufficient.

3.2 Model Build Verification

Once a model is designed and fabricated, it is important to understand the geometric differences between the as-built model and the reference configuration in order to gain confidence in the accuracy in both the model and the experimental results obtained. Given the importance of accuracy and repeatability within the CRM-HL ecosystem, it is recommended that models are manufactured and verified to a tight tolerance. However, because different test campaigns may have different test requirements (for example, a low Reynolds number test may require less shape accuracy when compared to a high Reynolds number test), no global manufacturing tolerance is provided. As an example, the Boeing 6% model is manufactured with a ± 0.003 " tolerance on the leading edge, which is in-line with the ± 0.003 " tolerance achieved on the ONERA LRM, but more relaxed compared to the ± 0.0015 " tolerance required for the NASA 5.2% model tested up to flight Reynolds numbers. It is also not possible to capture all important characteristics with a simple tolerance, as if one bounces from one extreme to another around a tight radius, there could be significant aerodynamic differences due to the local curvature changes. Surface finish requirements can also be critical, but aren't specified within the context of the ecosystem. These again are left to facility specific best practices, as the requirements may deviate based on expected Reynolds number. Beyond providing shape tolerances and surface finish requirements, it is recommended to conduct verification scans of the geometry, and to physically measure key quantities of interest such as slat at flap gaps, as described in the sections below.

3.2.1 Geometry Scan

Since full model part tolerances may be difficult to accurately assess, a geometrical inspection of both individual parts as they are manufactured, as well as the fully assembled model is recommended. While it is not the intention of the paper to go into details on specific measurement techniques, most models built to date have been verified by a mobile 3D measuring arm (typically a Faro® measurement system). A typical scan of assembled geometry is shown in Figure 13, where deviations are shown in model-scale inches.

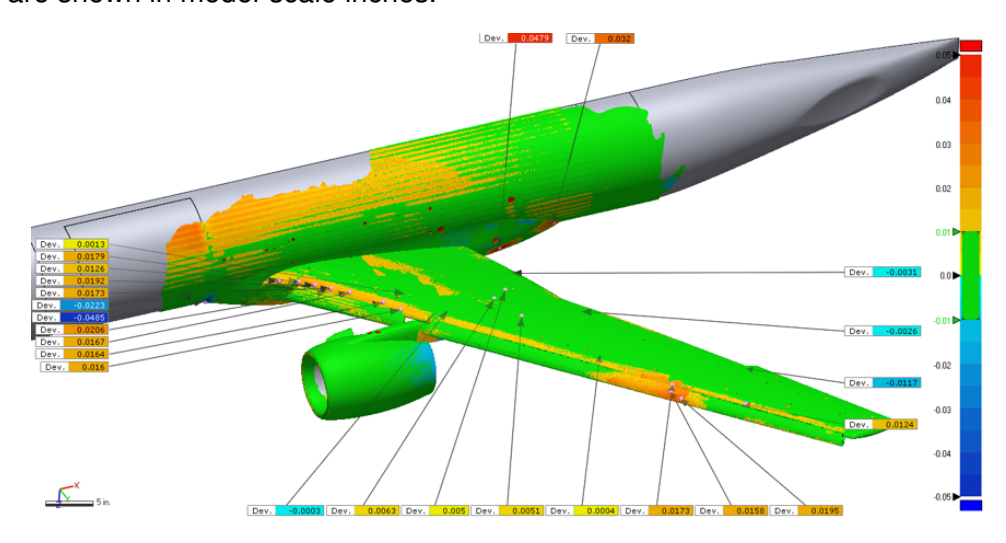


Figure 13 – 3d Assembled Model Scan of the NASA 5.2% model

Typically, parts are first checked to satisfy shape tolerances individually, then as a built-up assembly where positioning tolerance is determined. While the acceptability of an individual part is required to meet the specified manufacturing tolerances, often the positioning tolerance is a bit subjective and often facility or use case dependent. For a typical high lift configuration, the position of the leading edge slats and trailing edge flaps are critically important factors in aerodynamic performance, which in turn means consistency becomes a key driver in repeatability. Parameters of importance include deflection angle, gap between the device and the main element, and either the height above the WRP or overlap as defined by Lacy [5], and shown in Figure 14. These quantities can be derived from the points obtained in a 3D scan and are recommended to meet the good-practice requirements provided in Table 7. It is often required to manufacture at least minimal adjustability into device brackets in order to meet these stringent positioning requirements.

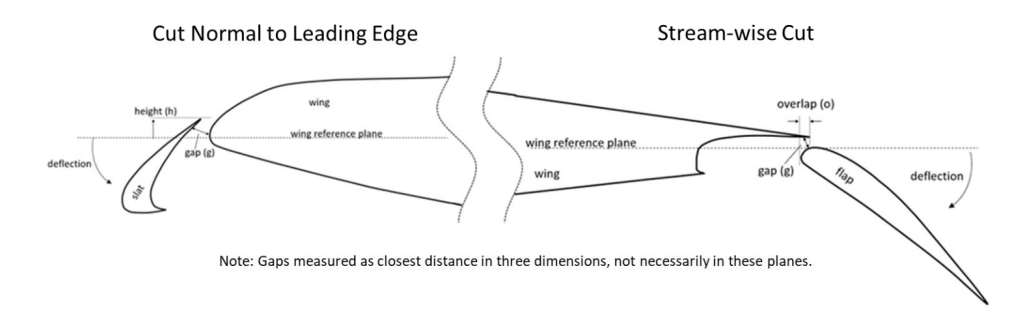


Figure 14 – Leading and Trailing Edge Device Positioning Parameters

3.2.2 Device Positioning Verification

In order to achieve better on-test repeatability, measurements of the device positioning quantities of interest can be made directly, instead of deriving device positioning from a 3D scan which

Table 7 – Good Practice Device Positioning Tolerances

Slat Deflection 0.25°
Slat Gap 0.03% MAC
Slat Height 0.03% MAC
Flap Deflection 0.25°
Flap Gap 0.02% MAC
Flap Overlap 0.03% MAC

involves specialized equipment and a lengthy measurement and interpretation process. Gap is perhaps easiest to measure, and can be directly checked with sufficiently accurate pin gauges. Direct measurements of both deflection and height or overlap require considerations during model design in order to precisely locate the relevant reference locations such as the wing reference plane or the spoiler trailing edge, but again can be made directly. Likewise, deflection measurements require an inclinometer and specialized tooling that can attach to the slat in some known orientation.

Here, the exact definitions of these measurements are important. Gap is defined as the 3D distance from a device to the closest wing surface. Slat height is the height of the slat trailing edge above the wing reference plane in the Z direction in the wing coordinate system. Flap overlap is the distance from the flap leading edge to the wing (or spoiler) trailing edge, measured in the X direction in wing coordinate system. Slat deflection angle is the component of rotation about the Y-axis of the leading edge coordinate system. Flap deflection angle is the component of rotation about the Y-axis of the wing coordinate system. Note: actual angles measured on physical model parts with an inclinometer are a function of (and can be corrected for) the feature being measured and the orientation of the part relative to the gravity vector (e.g. with or without dihedral).

If a model is designed for direct measurement, it is recommended that device positioning be verified to match the reference configuration after model setup is changed. If device positioning measurement considerations aren't made during the design process, it is recommended to physically measure device gap after model setup changes at a minimum. Device positioning values are given in Appendix B, and are provided coincident to bracket locations, with the exception of the inboard flap, which is provided adjacent to the fuselage. In many instances, flap support fairings will interfere with the measurement of overlap at the bracket centerline. In this instance, alternative overlap values at a location that can be measured should be extracted from the reference CAD.

4. Development of CFD Geometry

Since the primary objective of the CRM-HL ecosystem is aimed at CFD validation studies, a discussion on generating consistent geometry specifically for CFD is warranted. Typical high lift wind-tunnel models consist of specific parts and/or sub-assemblies to simplify manufacturing and to make rapid configuration changes feasible. Commonly there are part seams in many locations on the wing, brackets that separately attach into pockets on the wing and hold the leading and trailing edge devices in place, routing for instrumentation, hollow cavities inside of the fuselage, and even exposed fasteners in non-intrusive locations. To illustrate these complexities, an example of a slat and slat bracket part assembly for a CRM-HL model is shown in Figure 15. All of these complex model features are necessary to enable robust test campaigns within the ecosystem, but unfortunately make the development of accurate geometry for CFD challenging.

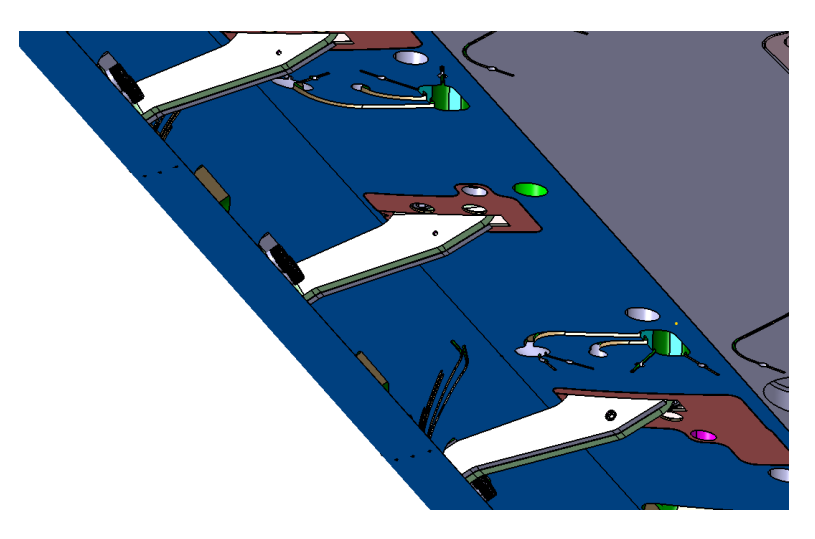


Figure 15 - Typical Slat Bracket Definition on the Boeing 6% CRM-HL

Given the desire to perform focused CFD validation through international aerospace community workshops and collaborations, establishing consistent computational geometry is paramount for consistent CFD analysis. If CFD model geometric simplifications are performed ad hoc by the engineer running the CFD simulation, then there is a risk that the uncertainty due to model simplification approaches may outweigh the model to model differences of interest. As a result, standard CFD geometry CAD files have been created (similar to geometry files created for the Reference configuration) for a number of CRM-HL wing tunnel models of interest, including the ONERA LRM-HL model and the NASA 5.2% model (both used in both HLPW-4 and HLPW-5). Figure 16 shows the same slat bracket geometry shown in Figure 15, but greatly simplified for CFD analysis, where fastener holes, part breaks, and instrumentation routing are all removed.

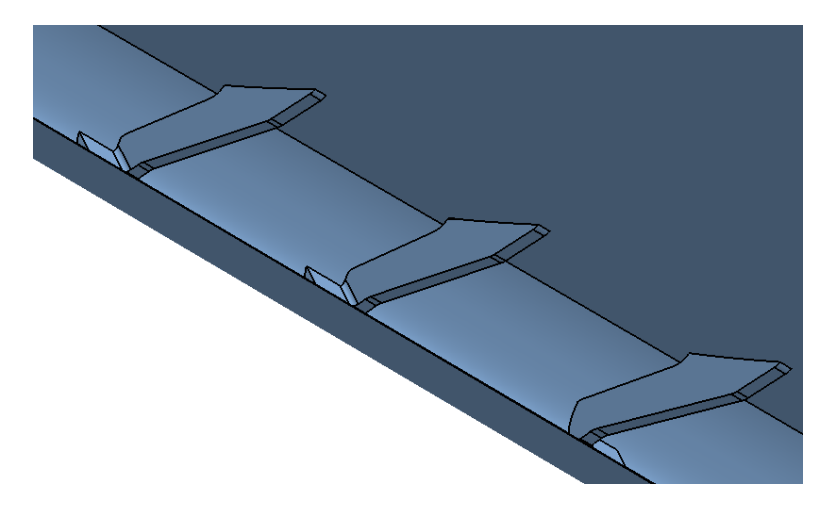


Figure 16 - Slat Brackets on the Boeing 6% CRM-HL Simplified for CFD

4.1 Computational Geometry Development Process

The process followed to generate model specific computational geometry generally begins with the assembled reference geometry provided within the NASA CRM website [2]. While the assembled geometry available to download is in generic STEP format, the working models are built in Dassault Systemes CATIA. The reference CAD model is built up from the CRM-HL ecosystem reference surfaces and retains the flexibility to parametrically adjust device positioning and turn off components to obtain the build-up configurations all within the same CAD model. This approach guarantees consistency in computational geometry across all CRM-HL configurations since they are all exported from the same source CAD model.

To build a wind tunnel model-specific computational geometry that reflects unique parts such as slat brackets, which may not be fully defined in the reference geometry, two approaches are generally considered. First, as-designed CAD can be simplified from an assembly level. While this approach is completely valid, the end result will be a computational model that more closely reflects the physical wind tunnel model, meaning that the wing surface may be split identically to where part breaks need to exist in the physical model. If this were done individually by each model manufacturer, there would be significant differences in topology between CFD models, resulting in differences driven into the computational grids and solutions. Further, with the wide variety of CAD systems in use across the world, this approach often results in the reference loft definitions translated between different CAD systems several times, potentially introducing losses in fidelity that cannot be easily controlled.

A second approach adopted here is to first closely compare the assembled reference models to the wind tunnel model specific as-designed assembly. Since all ecosystem wind-tunnel models are defined from the same source lofts, this comparison is generally straight forward. During this comparison, unique parts are noted, then simplified and incorporated into the reference computational geometry. These unique parts are typically limited to slat brackets, flap track fairings, and any mounting pads necessary for model assembly, apart from the aerodynamic surface differences in earlier models discussed above. The end result in this approach is a consistent set of geometric models that fully reflect each unique wind-tunnel model, but are simplified and suitable for CFD and of near identical architecture to the reference geometry.

In addition to the machined parts, a number of adjustments to the computational model are further required to address the on-test device sealing that is typically done. Section 2.3 describes one of the largest modifications, which is the addition of the flap to flap sealing. This sealing is typically performed with tape and filler, which in turn means a CAD definition is unavailable. Sealing in the provided CFD models is defined to match the size specifications provided, and does not attempt to match exact shapes achieved with filler.

Sometimes modifications are necessary to the computational geometry to enable proper grid building. One typical modification that is performed is to close very small gaps between the slats and their matching trim planes on the wing (orange colored surface in Figure 17). In this region, clearance is typically added to ease physical part assembly and allow adjustability without interference, but is best sealed by extending the slat into the orange surface to simplify CFD grid generation. The extension required to fully seal the slat edge to the wing in this area is typically less than 0.1" full-scale, and can be shown to be aerodynamically insignificant.

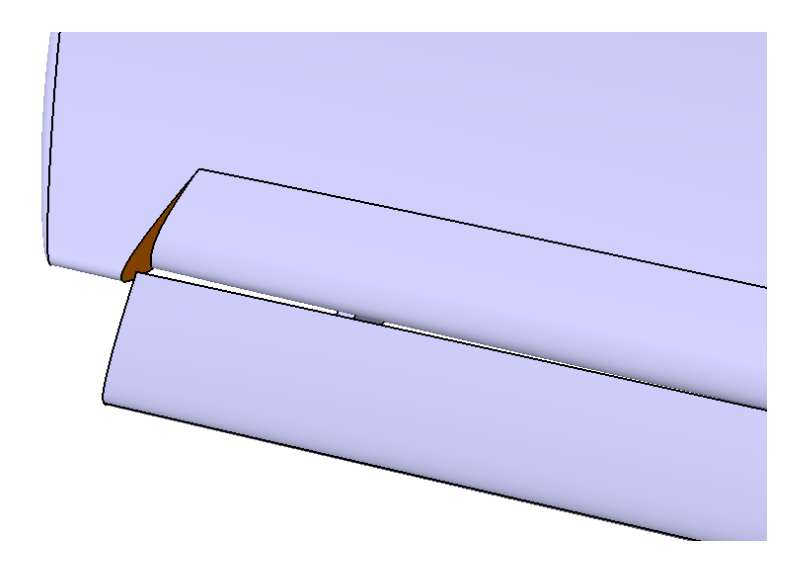


Figure 17 – Slat Modelling for CFD is Typically Extended to Orange Surface

Lastly, there is a general desire in the community to perform CFD analysis on as-built geometry

rather than using the as-designed geometry procedure described above. Some attempts have been made to identify and account for gross positioning errors that may be introduced in the fabrication process, but minimal effort has been spent to adjust the underlying surface contours to reflect required geometry changes, if any. To this point, it is challenging to both adequately align 3D scan data with the reference geometry surfaces, and incorporate any required surface deviations into the underlying CAD geometry in a meaningfully accurate manner. Based on experience, the authors believe that a part machined using facility best practice tolerances is sufficient, making the deviations described here a second-order effect particularly relative to the aeroelastic variations that occur under load.

5. Conclusions

With a growing number of wind-tunnel models available for testing, maintaining consistent geometry across the extensive CRM-HL ecosystem presents a unique challenge that is well beyond the scope of the original transonic CRM. Careful considerations are described in this paper to verify and ensure that all wind tunnel test articles are indeed faithful representations of the original reference geometry. These include providing and documenting guidance on device sealing that was not originally defined, and documenting specific guidance on geometry processing previously provided via less formal means. Additional methods of verifying leading and trailing edge device positioning are also described, with the intent that users of wind-tunnel models will consistently check and document positioning before collecting test data. All of these details are aimed at enabling consistent models and increasing confidence in the experimental results. In order to achieve this confidence and consistency, it is an expectation that model geometry validation per these practices is performed on all configurations used within the ecosystem.

Further details are provided on modifications of the reference geometry that can be used to either run simulations on a simplified configuration, or used to compare against designed CAD parts for testing. A process is also shared on generation of consistent geometry for use in CFD modeling. Outlining and documenting these processes will enable the creation of consistent CFD models representing wind tunnel models which are either being fabricated or considered for construction, ensuring that any new models are consistent with those that already exist.

6. Contact Author Email Address

adam.m.clark@boeing.com

7. Copyright Statement

At least one, but possibly not all, of the authors of the Work is an employee of The Boeing Company or one of its wholly-owned subsidiaries ("BOEING") who prepared the Work within the scope of his or her employment. The Boeing employee(s) listed above are not authorized to assign or license Boeing's rights to the Work, or otherwise bind Boeing. However, subject to the limitations set forth below, Boeing is willing to assign its copyright in the Work to Publisher.

Notwithstanding any assignment or transfer to the Publisher, or any other terms of this Agreement, the rights granted by Boeing to Publisher are limited as follows: (i) any rights granted by Boeing to the Publisher are limited to the work-made-for-hire rights Boeing enjoys in the Work; (ii) Boeing makes no representation or warranty of any kind to the Publisher or any other person or entity regarding the Work, the information contained therein, or any related copyright; and (iii) Boeing retains a non-exclusive, perpetual, worldwide, royalty-free right, without restriction or limitation, to use, reproduce, publicly distribute, display, and perform and make derivative works from the Work, and to permit others to do so.

References

- [1] D. S. Lacy and A. J. Sclafani, "Development of the high lift common research model (HL-CRM): A representative high lift configuration for transports." *AIAA Paper 2016-0308.*, 2016.
- [2] M. Rivers, "CRM-HL Geometry | NASA Common Research Model," 2022, last accessed 21 June 2024. [Online]. Available: https://commonresearchmodel.larc.nasa.gov/high-lift-crm/high-lift-crm-geometry/
- [3] J. C. Lin, L. P. Melton, J. A. Hannon, M. Y. Andino, M. Koklu, K. B. Paschal, and V. N. Vatsa, "Testing of High-Lift Common Research Model with Integrated Active Flow Control," *Journal of Aircraft*, vol. 57, no. 6, pp. 1121–1133, 2020. [Online]. Available: https://doi.org/10.2514/1.C035906
- [4] A. N. Evans, D. S. Lacy, I. Smith, and M. B. Rivers, "Test Summary of the NASA High-Lift Common Research Model Half-Span at QinetiQ 5-Metre Pressurized Low-Speed Wind Tunnel." *AIAA Paper 2020-2770.*, 2020.
- [5] D. S. Lacy and A. M. Clark, "Definition of Initial Landing and Takeoff Reference Configurations for the High Lift Common Research Model (CRM-HL)." *AIAA Paper 2020-2771.*, 2023.
- [6] G. C. Sylvain Mouton and A. Lorenski, "Test Summary of the Full-Span High-Lift Common Research Model at the ONERA F1 Pressurized Low-Speed Wind Tunnel." *AIAA Paper 2023-0823.*, 2023.
- [7] J. C. Vassberg, M. A. DeHaan, S. M. Rivers, and R. A. Wahls, "Development of a Common Research Model for Applied CFD Validation Studies." *AIAA Paper 2008-6919*., 2023.
- [8] C. L. Rumsey, J. P. Slotnick, and C. Woeber, "HLPW-4/GMGW-3: Overview and Workshop Summary." *AIAA Paper 2022-3295.*, 2022. [Online]. Available: https://arc.aiaa.org/doi/abs/10.2514/6.2022-3295

A Reference Pressure Belt Locations

Reference wing pressure belts are defined and named as shown in figure 18, including the eta span locations (for reference only). Actual pressure belt locations are defined to be in-plane with the wing coordinate system Y-axis, but are 'kinked' to be perpendicular to the leading edge forward of the wing quarter chord. Plane coefficients are provided in Table 8 that satisfy the equation Ax + By + Cz = D. A single pressure belt is defined by the wing LE belt (eg. LEA) forward of the quarter chord, and the wing belt (eg. WA) aft, where the quarter chord is defined as the intersection of the two planes.

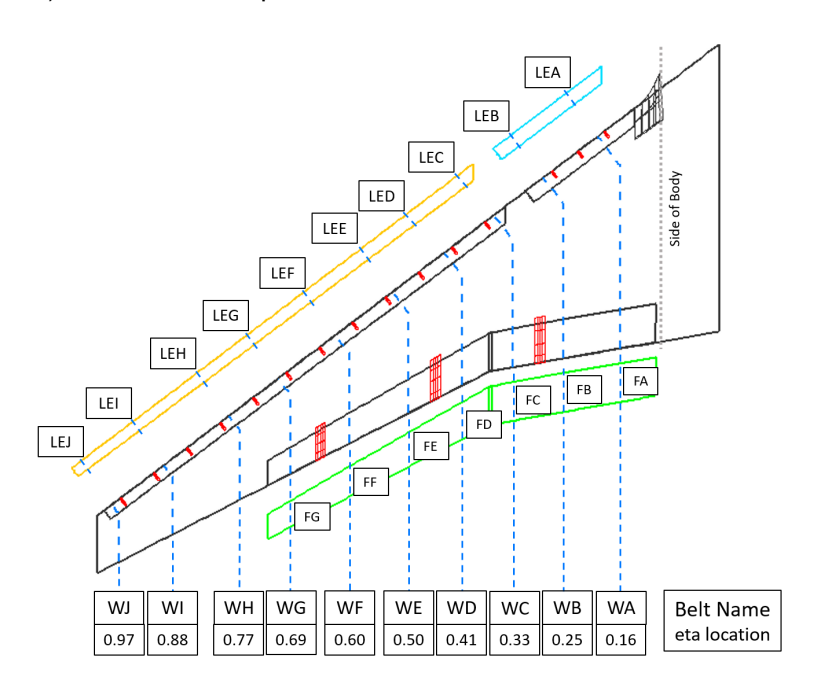


Figure 18 – Reference Pressure Belt Names

Table 8 – Wing Pressure Belt Locations

Wing Belt	Α	В	С	D
WA	0.000	1.000	0.000	185.0000
WB	0.000	1.000	0.000	290.0000
WC	0.000	1.000	0.000	385.0000
WD	0.000	1.000	0.000	480.0000
WE	0.000	1.000	0.000	580.0000
WF	0.000	1.000	0.000	690.0000
WG	0.000	1.000	0.000	800.0000
WH	0.000	1.000	0.000	895.0000
WI	0.000	1.000	0.000	1020.0000
WJ	0.000	1.000	0.000	1120.0000
LEA	0.604356	-0.796714	0.000000	284.3966
LEB	0.604356	-0.796714	0.000000	412.3192
LEC	0.604356	-0.796714	0.000000	528.0587
LED	0.604356	-0.796714	0.000000	643.7981
LEE	0.604356	-0.796714	0.000000	765.6291
LEF	0.604356	-0.796714	0.000000	899.6432
LEG	0.604356	-0.796714	0.000000	1033.6573
LEH	0.604356	-0.796714	0.000000	1149.3968
LEI	0.604356	-0.796714	0.000000	1301.6856
LEJ	0.604356	-0.796714	0.000000	1423.5166

B Leading and Trailing Edge Device Positioning Verification

Table 9 - Inboard Slat Landing Positions (full-scale Inches)

Bracket	1	2	3
LES Location Deflection	269.63	331.09 30	392.54
Gap Height (Above WRP)		3.8107 3.2823	3.5613 3.9351

Table 10 – Mid-Span Slat Landing Positions (full-scale Inches)

Bracket	4	5	6	7	8	9
LES Location	549.39	627.01	704.63	782.25	859.86	937.48
Deflection 3				0		
Gap	3.1476	3.1031	3.1078	3.1195	3.1199	3.0986
Height (Above WRP)	4.4251	3.9002	3.3768	2.8503	2.3245	1.7958

Table 11 – Outboard Slat Landing Positions (full-scale Inches)

Bracket	10	11	12	13	14	15
LES Location	549.39	627.01	704.63	782.25	859.86	937.48
Deflection				30		
Gap	3.0525	2.9845	2.9060	2.9020	3.0145	2.8426
Height (Above WRP)	1.2637	0.7278	0.2058	-0.2662	-0.7281	-1.4461

Table 12 – Inboard Slat Takeoff Positions (full-scale Inches)

Bracket	1	2	3
LES Location	269.63	331.09	392.54
Deflection		30	
Gap	0.00	0.00	0.00
Height (Above WRP)	6.0914	6.4671	6.8405

Table 13 – Mid-Span Slat Takeoff Positions (full-scale Inches)

Bracket	4	5	6	7	8	9
LES Location	549.39	627.01	704.63	782.25	859.86	937.48
Deflection	30					
Gap	0.00	0.00	0.00	0.00	0.00	0.00
Height (Above WRP)	6.9114	6.3720	5.8342	5.2932	4.7527	4.2092

Table 14 – Outboard Slat Takeoff Positions (full-scale Inches)

Bracket	10	11	12	13	14	15
LES Location	549.39	627.01	704.63	782.25	859.86	937.48
Deflection	30					
Gap	0.00	0.00	0.00	0.00	0.00	0.00
Height (Above WRP)	3.6622	3.1110	2.5748	2.0919	1.6201	0.8740

Table 15 – Inboard Flap Takeoff Positions (full-scale Inches)

Deflection	1	0	25		
Bracket	IB OB		IB	OB	
Gap Overlap	1.2806 20.6906	1.3855 20.8419	2.5799 10.7973	2.6259 9.3831	

Table 16 – Inboard Flap Landing Positions (full-scale Inches)

	37		•	0	43	
Bracket	IB	ОВ	IB	OB	IB	OB
Gap Overlap	2.8774	2.8037	2.8785	2.8507	2.8798 5.3674	2.8857
Overlap	5.3000	2.0234	5.3772	2.5656	5.3674	2.301

Table 17 – Outboard Flap Takeoff Positions (full-scale Inches)

Deflection	1	0	25		
Bracket	IB OB		IB	ОВ	
Gap	1.2500	0.9426			
Overlap	18.9218	14.9454	8.3820	6.5798	

Table 18 – Outboard Flap Landing Positions (full-scale Inches)

Deflection			3	7	40	
Bracket	IB	OB	IB	ОВ	IB	OB
Gap Overlap	2.5955	2.0831	2.6214	2.1015	2.6523	2.1222
Overlap	2.5690	1.9851	2.5690	1.9851	2.5690	1.9851